

Search for the decay $K_L \rightarrow \pi^0 \nu \bar{\nu}$ using $\pi^0 \rightarrow e^+ e^- \gamma$

A. Alavi-Harati,¹² I. F. Albuquerque,¹⁰ T. Alexopoulos,¹² M. Arenton,¹¹ K. Arisaka,² S. Averitte,¹⁰ A. R. Barker,⁵ L. Bellantoni,⁷ A. Bellavance,⁹ J. Belz,¹⁰ R. Ben-David,⁷ D. R. Bergman,¹⁰ E. Blucher,⁴ G. J. Bock,⁷ C. Bown,⁴ S. Bright,⁴ E. Cheu,¹ S. Childress,⁷ R. Coleman,⁷ M. D. Corcoran,⁹ G. Corti,¹¹ B. Cox,¹¹ M. B. Crisler,⁷ A. R. Erwin,¹² R. Ford,⁷ A. Glazov,⁴ A. Golossanov,¹¹ G. Graham,⁴ J. Graham,⁴ K. Hagan,¹¹ E. Halkiadakis,¹⁰ K. Hanagaki,^{8,*} M. Hazumi,⁸ S. Hidaka,⁸ Y. B. Hsiung,⁷ V. Jejer,¹¹ J. Jennings,² D. A. Jensen,⁷ R. Kessler,⁴ H. G. E. Kobrak,³ J. LaDue,⁵ A. Lath,¹⁰ A. Ledovskoy,¹¹ P. L. McBride,⁷ A. P. McManus,¹¹ P. Mikelsons,⁵ E. Monnier,^{4,†} T. Nakaya,⁷ U. Nauenberg,⁵ K. S. Nelson,¹¹ H. Nguyen,⁷ V. O'Dell,⁷ M. Pang,⁷ R. Pordes,⁷ V. Prasad,⁴ C. Qiao,⁴ B. Quinn,⁴ E. J. Ramberg,⁷ R. E. Ray,⁷ A. Roodman,⁴ M. Sadamoto,⁸ S. Schnetzer,¹⁰ K. Senyo,⁸ P. Shanahan,⁷ P. S. Shawhan,⁴ W. Slater,² N. Solomey,⁴ S. V. Somalwar,¹⁰ R. L. Stone,¹⁰ I. Suzuki,⁸ E. C. Swallow,^{4,6} R. A. Swanson,³ S. A. Taegar,¹ R. J. Tesarek,¹⁰ G. B. Thomson,¹⁰ P. A. Toale,⁵ A. Tripathi,² R. Tschirhart,⁷ Y. W. Wah,⁴ J. Wang,¹ H. B. White,⁷ J. Whitmore,⁷ B. Winstein,⁴ R. Winston,⁴ J.-Y. Wu,⁵ T. Yamanaka,⁸ and E. D. Zimmerman⁴

¹ University of Arizona, Tucson, Arizona 85721

² University of California at Los Angeles, Los Angeles, California 90095

³ University of California at San Diego, La Jolla, California 92093

⁴ The Enrico Fermi Institute, The University of Chicago, Chicago, Illinois 60637

⁵ University of Colorado, Boulder, Colorado 80309

⁶ Elmhurst College, Elmhurst, Illinois 60126

⁷ Fermi National Accelerator Laboratory, Batavia, Illinois 60510

⁸ Osaka University, Toyonaka, Osaka 560 Japan

⁹ Rice University, Houston, Texas 77005

¹⁰ Rutgers University, Piscataway, New Jersey 08855

¹¹ The Department of Physics and Institute of Nuclear and Particle Physics, University of Virginia, Charlottesville, Virginia 22901

¹² University of Wisconsin, Madison, Wisconsin 53706

(Received 8 July 1999; published 10 March 2000)

We report on a search for the decay $K_L \rightarrow \pi^0 \nu \bar{\nu}$, carried out as a part of E799-II, a rare K_L decay experiment at Fermilab. Within the standard model, the $K_L \rightarrow \pi^0 \nu \bar{\nu}$ decay is dominated by direct CP violating processes, and thus an observation of the decay implies confirmation of direct CP violation. No events were observed, and we set an upper limit for the branching ratio of $K_L \rightarrow \pi^0 \nu \bar{\nu}$ to be $< 5.9 \times 10^{-7}$ at the 90% confidence level.

PACS number(s): 13.20.Eb, 11.30.Er, 12.15.Hh

I. INTRODUCTION

The decay $K_L \rightarrow \pi^0 \nu \bar{\nu}$ is dominated by direct CP violating processes within the standard model through second order diagrams such as Z penguin diagrams [1]. Indirect CP violating and CP conserving contributions are expected to be highly suppressed [2–5] for the following reasons. First order decay diagrams, which lead to relatively large indirect CP violation in $K_L \rightarrow \pi\pi$, do not contribute to $K_{L,S} \rightarrow \pi^0 \nu \bar{\nu}$ because of the absence of a tree level flavor changing neutral current. The indirect CP violating contribution via second order diagrams is suppressed by five orders of magnitude (ϵ^2). Long-distance indirect CP violating and CP conserving contributions from $K_L \rightarrow \pi^0 \gamma^*$ and $K_L \rightarrow \pi^0 \gamma^* \gamma^*$ intermediate states, which are significant in $K_L \rightarrow \pi^0 e^+ e^-$ and $K_L \rightarrow \pi^0 \mu^+ \mu^-$, do not exist in $K_L \rightarrow \pi^0 \nu \bar{\nu}$ because the neutrinos in the final state do not couple to virtual photons [6].

Following the Wolfenstein parametrization of the

Cabibbo-Kobayashi-Maskawa (CKM) matrix [7,8], the branching ratio $B(K_L \rightarrow \pi^0 \nu \bar{\nu})$ is proportional to η^2 . The uncertainty of the hadronic matrix element in $K_L \rightarrow \pi^0 \nu \bar{\nu}$ is eliminated by the experimental measurement of $\Gamma(K^+ \rightarrow \pi^0 e^+ \nu)$ and the lifetime of K_L , which leads to an uncertainty of $\pm 1.5\%$ in the expectation of $B(K_L \rightarrow \pi^0 \nu \bar{\nu})$. In addition, due to the small uncertainty ($\sim 3\%$) in the next-to-leading order QCD correction [9], $B(K_L \rightarrow \pi^0 \nu \bar{\nu})$ gives direct access to η . The current knowledge of the CKM parameters [10] allows us to predict $B(K_L \rightarrow \pi^0 \nu \bar{\nu})$ to be $(1-5) \times 10^{-11}$ [11]. The uncertainty comes directly from the input CKM parameters. As the theoretical calculations are unambiguous, an observation of the decay $K_L \rightarrow \pi^0 \nu \bar{\nu}$ at the sensitivity of $\sim 10^{-11}$ would indicate the existence of direct CP violation, and an observation outside the predicted range would indicate new physics [12].

It is experimentally difficult to search for $K_L \rightarrow \pi^0 \nu \bar{\nu}$ because the signature is only an isolated π^0 . The current upper limit, $B(K_L \rightarrow \pi^0 \nu \bar{\nu}) < 1.6 \times 10^{-6}$ at the 90% confidence level, was obtained by using $\pi^0 \rightarrow \gamma\gamma$ decay [13]. We report on the search for $K_L \rightarrow \pi^0 \nu \bar{\nu}$ in the Dalitz decay mode (π^0

*To whom correspondence should be addressed. kazu@fnal.gov

†On leave from C.P.P. Marseille/C.N.R.S., France

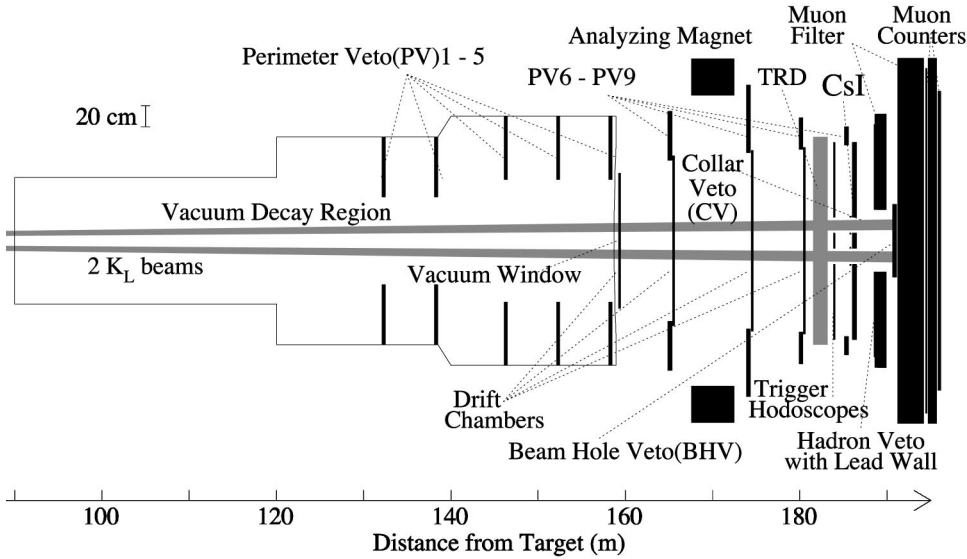


FIG. 1. KTeV detector configuration for E799-II.

$\rightarrow e^+e^-\gamma, \pi_D^0$) with the E799-II experiment using the KTeV detector at Fermilab. The data were collected in 44 days of running in 1997.

II. THE APPARATUS

Figure 1 shows a plan view of the KTeV detector. The elements of the detector relevant to this search are described below. Kaons were produced by an 800 GeV proton beam that struck a 30 cm long BeO target with a cross section of $3 \text{ mm} \times 3 \text{ mm}$ at a targeting angle of 4.8 mrad. In the first (second) part of the running period, two neutral side-by-side beams with a solid angle of 0.25 (0.35) μsr each were defined by collimators downstream of the target. A 7.6 cm long lead absorber was placed to convert photons in the beams to electron-positron pairs which would be removed by the sweeping magnets located downstream of the target. The two beams entered a 69 m long evacuated (10^{-5} – 10^{-6} torr) decay volume starting 90 m from the target. The downstream end of the volume was sealed by a vacuum window made of Kevlar and Mylar with a thickness of 0.0035 radiation lengths (X_0) in total [14]. The neutral beam was mainly composed of neutrons, K_L 's, Λ^0 's, and Ξ^0 's with the relative ratios of 3.5 : 1 : 0.02 : 7.5×10^{-4} at the beginning of the vacuum decay region. The average kaon momentum was 70 GeV/c. Approximately 3% of the kaons decayed inside the vacuum decay region.

The position and momentum of charged particles were measured using a spectrometer consisting of four drift chambers, two upstream and two downstream of a dipole analyzing magnet. The magnet had a momentum kick of 205 MeV/c. Each chamber consisted of two orthogonal views (x and y), and had approximately 100 μm single-hit position resolution per view. An electromagnetic calorimeter with dimensions of $1.9 \text{ m} \times 1.9 \text{ m}$ and $27 X_0$ in depth was used for photon detection and electron identification [15]. It was composed of 3100 pure CsI crystals. The energy resolution of the calorimeter was below 1% averaged over the electron energy range 2 to 60 GeV. A scintillator hodoscope was placed just

upstream of the calorimeter for charged particle triggering. There were 8 transition radiation detectors (TRD's) between the spectrometer and the trigger hodoscope for e/π separation. The TRD's consisted of polypropylene fiber mats as radiators and active multiwire proportional chamber (MWPC) volumes.

The hermetic photon veto system, consisting of perimeter vetoes (PV) 1–9, a collar veto (CV) and a beam hole veto (BHV), was used to detect photons missing the fiducial area of the calorimeter. Each photon veto counter had a sandwich structure of Pb (W in the CV) and scintillator. The total depth of radiator was $16 X_0$ for PV's, $8.6 X_0$ for CV, and $30 X_0$ (equivalent to ~ 1 nuclear interaction length) for BHV. The BHV was located downstream of the calorimeter and in the neutral beam region. The BHV was segmented into two transverse sections (one per beam) and three longitudinal sections ($10 X_0$ each). Downstream of the calorimeter, there was a 10 cm lead wall followed by a scintillator plane (hadron veto) to reject charged pions.

The trigger was designed to accept events with two electrons and a photon so that $K_L \rightarrow \pi_D^0 \nu \bar{\nu}$ and $K_L \rightarrow e^+e^-\gamma$ decays were accepted. The $K_L \rightarrow e^+e^-\gamma$ decays were used to measure the number of decayed K_L 's. The trigger hodoscope and drift chambers were used to select two charged track events. The calorimeter was required to have an energy deposit greater than 18 (24) GeV in the first (second) part of the running period. Events with significant energy in the photon or hadron vetoes were rejected. Events with three or four clusters in the calorimeter with a minimum energy of 1 GeV were selected by the hardware cluster counting system [16]. The TRD pulse height information was used to identify electrons at the trigger level.

III. EVENT SELECTION

The strategy in offline selection was to identify π_D^0 decays by reconstructing the invariant mass ($m_{ee\gamma}$) and selecting high p_t events in order to suppress backgrounds, where p_t is a total momentum transverse to the K_L flight direction. The

K_L direction was measured as a vector projected from the target to the decay vertex point on an event-by-event basis. The p_t cut was used because π^0 's from $K_L \rightarrow \pi^0 \nu \bar{\nu}$ have a higher kinematic p_t limit than those from most of background processes.

In order to avoid human bias in the determination of selection criteria, a blind analysis was performed. A masked region was defined in the p_t vs $m_{ee\gamma}$ plane as $125 < m_{ee\gamma}(\text{MeV}/c^2) < 145$ and $160 < p_t(\text{MeV}/c) < 240$. Monte Carlo (MC) simulation was used to optimize all cuts while data within the masked region were hidden.

The offline event selection began with the identification of π_D^0 decays by requiring $125 < m_{ee\gamma}(\text{MeV}/c^2) < 145$ ($\sim \pm 3\sigma$). There were five categories in the remaining backgrounds such as $K_L \rightarrow \pi^\pm e^\mp \nu$ (K_{e3}), $K_L \rightarrow \pi^+ \pi^- \pi_D^0$, hyperon decays, $K_L \rightarrow \pi^0 \pi_D^0$, $K_L \rightarrow \pi^0 \pi^0 \pi_D^0$, and beam background. Below we describe the cuts to suppress each background.

A serious background was K_{e3} decays where a photon was radiated from the electron or overlapped accidentally, and the pion was misidentified as an electron. Electrons were selected by requiring $0.95 < E/p < 1.05$ where E is the energy deposited in the calorimeter and p is the momentum measured by the spectrometer. This cut was 94% efficient for detecting both electrons and 0.4% for a pion. The transverse shower shape at the calorimeter was also used to distinguish electrons from pions. The confidence level to identify pions formed from the 8 TRD's was required to be less than 1%, which gave a 95.0% efficiency for electrons. Events with out-of-time accidental energy in the calorimeter were rejected. The photon energy was required to be greater than 3 GeV because accidental and radiated photons typically have lower energy. Dalitz decays, which favor low m_{ee} , were selected by requiring $m_{ee}/m_{ee\gamma} < 0.3$, where m_{ee} is the invariant mass of the electron pair. Defining θ_+ (θ_-) as the angle between a photon and a positron (electron) in the π^0 's rest frame, $\cos \theta_+ + \cos \theta_-$ was required to be less than -1.5 , because π^\pm and e^\mp in semileptonic decays prefer a wide opening angle. These two kinematic cuts rejected 99.6% of K_{e3} events with a signal efficiency of 78%.

Backgrounds involving π_D^0 decays with unreconstructed charged particles, such as $K_L \rightarrow \pi^+ \pi^- \pi_D^0$, were suppressed by eliminating events with more activity in the drift chambers than expected from two charged track events.

High momentum, typically 200 to 300 GeV/c, Λ^0 's and Ξ^0 's could reach the decay region. Decays of these hyperons could lead to backgrounds such as $\Lambda^0 \rightarrow n \pi_D^0$ and $\Xi^0 \rightarrow \Lambda^0 \pi_D^0$, because of the undetected neutrons, or protons and pions. These backgrounds were reduced by requiring the z position, or decay distance from the target, to be greater than 120 m. Since hyperons had higher energy than kaons, events with photon energy greater than 50 GeV were rejected. To suppress backgrounds with neutrons such as $\Lambda^0 \rightarrow n \pi_D^0$, the energy deposited to the third segment of BHV was required to be less than 200 minimum ionizing particles equivalent. This cut was applied only for the $+x(-x)$ side of BHV when the decay vertex was found in the $+x(-x)$ region to minimize the signal loss due to accidental activity.

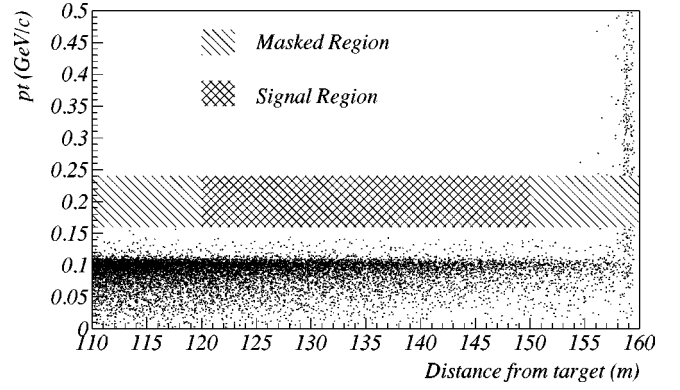


FIG. 2. p_t vs z before the p_t cut. The location of the vacuum window is $z = 159$ m.

The $K_L \rightarrow \pi^0 \pi_D^0$ and $K_L \rightarrow \pi^0 \pi^0 \pi_D^0$ backgrounds were suppressed by the photon veto system. The thresholds for measured photon energy were set to 200 MeV for PV1 and PV2, 250 MeV for PV3, 100 MeV for the rest of PV's, 1 GeV for CV, and 5 GeV (8.5 GeV) for the first section of BHV on the same (opposite) side as the reconstructed decay position. The number of clusters with energy greater than 1 GeV at the calorimeter was required to be three, and events with extra clusters with energy greater than 250 MeV were rejected. The photon veto requirements rejected 99.5% of $K_L \rightarrow \pi^0 \pi_D^0$ and over 99.99% of $K_L \rightarrow \pi^0 \pi^0 \pi_D^0$ events, while 41% of the signal, as measured by $K_L \rightarrow e^+ e^- \gamma$ events, was lost. The signal loss was mostly due to the high rate neutral beams (13 MHz K_L and 44 MHz neutron) striking the BHV. The rejection factor in the MC was compared with data by using events with $p_t < 150$ MeV/c and $m_{ee\gamma} < 100$ MeV/c². It is expected from MC that 84% of events were $K_L \rightarrow \pi^0 \pi^0 \pi_D^0$ or $K_L \rightarrow \pi^0 \pi_D^0$ or $\Xi^0 \rightarrow \Lambda^0 \pi_D^0$ in the kinematic region above. The fraction of events passing the photon veto requirements in this region was measured to be $1.0 \pm 0.4\%$ in real data, while $1.6 \pm 0.5\%$ in MC.

Another background was associated with π^0 's produced by beam interactions with detector materials, primarily the vacuum window, as shown in Fig. 2. There was a cluster of events at $z \approx 159$ m, the location of the vacuum window. To reject such events, the decay vertex position in z was required to be less than 150 m.

The remaining backgrounds were primarily from hyperon decays, which had a well-reconstructed π_D^0 decay in the fiducial region. These were rejected by requiring p_t to be $160 < p_t(\text{MeV}/c) < 240$ as shown in Fig. 3. The cut on the high end was determined from the kinematic limit of $K_L \rightarrow \pi^0 \nu \bar{\nu}$ decays, allowing for resolution. The main peak arose from $\Lambda^0 \rightarrow n \pi_D^0$, and the shoulder at 135 MeV/c was from $\Xi^0 \rightarrow \Lambda^0 \pi_D^0$. The MC events were normalized by the measured number of decayed K_L 's, Λ^0 's, and Ξ^0 's. With this absolute normalization, the agreement between data and MC distributions is excellent. Combining $m_{ee\gamma}$ and p_t cuts, the efficiency was less than 1.4×10^{-6} for $\Lambda^0 \rightarrow n \pi_D^0$, 4.5×10^{-5} for $\Xi^0 \rightarrow \Lambda^0 (\rightarrow p \pi^-) \pi_D^0$, 1.7×10^{-4} for $\Xi^0 \rightarrow \Lambda^0 (\rightarrow n \pi^0) \pi_D^0$, and 1.7% for $\Xi^0 \rightarrow \Lambda^0 (\rightarrow n \pi_D^0) \pi^0$, while the signal efficiency was 46%.

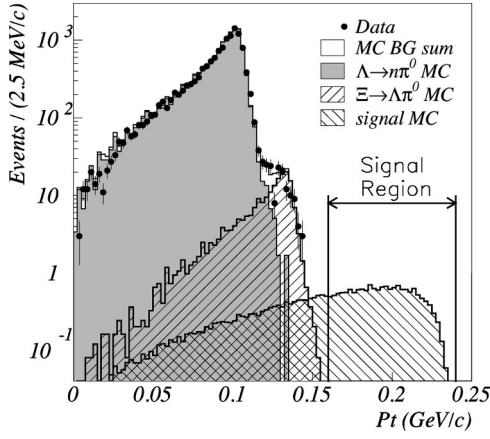


FIG. 3. Final p_t distribution. The dots represent data, and open histogram is for MC expectation. Two main background contributions are overlaid. Also shown is the signal distribution predicted from the MC simulation whose normalization is arbitrary.

IV. BACKGROUND ESTIMATION

The MC simulation played an important role in both the calculation of signal efficiency and the estimation of background level. Accidental events taken during the runs were embedded into the MC simulation for reproducing real events. In order to verify the MC simulation and our understanding of the backgrounds, events around the masked region were compared between data and MC expectation as shown in Fig. 4. The region (f), which had the largest discrepancy of all the regions, had a Poisson probability of 5.6% for observing 10 events when 6.5 events were expected. The good agreement between the expectation and the data in both the p_t shape and the number of events validates the MC simulation and our understanding of the backgrounds. Even if one or more of the cuts is relaxed, the agreement is still excellent.

The side band data were used in the background level

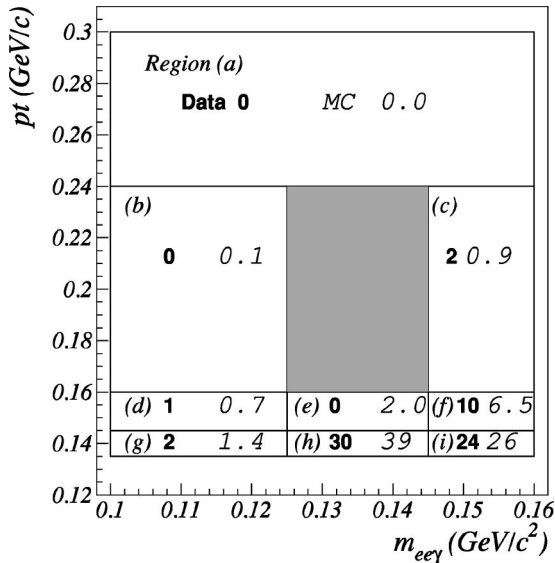


FIG. 4. Number of events around masked region. The left (bold) numbers represent data and the right (italic) is MC expectation.

TABLE I. Summary of expected background contribution in the final signal region.

Decay mode	Expected number of events
$K_L \rightarrow \pi e \nu + \gamma$	0.02 ± 0.02
$K_L \rightarrow \pi^+ \pi^- \pi_D^0$	< 0.01
$\Lambda \rightarrow n \pi_D^0$	< 0.04
$\Xi^0 \rightarrow \Lambda^0 (\rightarrow p \pi^-) \pi_D^0$	$0.01^{+0.006}_{-0.004}$
$\Xi^0 \rightarrow \Lambda^0 (\rightarrow n \pi^0) \pi_D^0$	$0.01^{+0.006}_{-0.004}$
$\Xi^0 \rightarrow \Lambda^0 (\rightarrow n \pi_D^0) \pi^0$	0.01 ± 0.01
$K_L \rightarrow \pi^0 \pi^0 \pi_D^0$	0.03 ± 0.03
$K_L \rightarrow \pi^0 \pi_D^0$	< 0.01
$n + X \rightarrow \pi^0 X'$	$0.04^{+0.04}_{-0.01}$
Total	$0.12^{+0.05}_{-0.04}$

estimation for beam interactions. We first looked at z distribution for the $p_t > 240$ MeV/c region, and estimated the contamination level into the signal range in z by fitting the z shape with exponential. As a result, 0.08 events were expected in the region $120 < z$ (m) < 150 and $p_t > 240$ MeV/c. Next we scaled down the size of background to $160 < p_t$ (MeV/c) < 240 range by fitting the p_t shape with $f(p_t) = \exp[\text{const} + \text{slope} \times p_t \text{ (GeV/c)}]$. As a result, 50% of the number of events in the $p_t > 240$ MeV/c region were expected to be in $160 < p_t$ (MeV/c) < 240 . The slopes in the exponential fitting of the p_t are -4.5 ± 0.3 , -4.5 ± 1.1 , -5.0 ± 1.6 , and -3.6 ± 4.4 in unit of $1/(\text{GeV/c})$ for z between 159 and 157 m with an interval of 0.5 m, respectively, and no correlation between p_t and z was found. Finally the contamination of backgrounds to the signal region due to beam interactions was estimated to be 0.04 ($= 0.08 \times 50\%$) events.

The background levels except for those from beam interactions were estimated by using the MC simulation, and summarized in Table I. In total, $0.12^{+0.05}_{-0.04}$ background events were expected.

V. ACCEPTANCE

The signal acceptance for K_L 's decaying between 90 and 160 m from the target and with a momentum range of 20 to 220 GeV/c was calculated from MC simulation to be 0.152%. The acceptance for $K_L \rightarrow e^+ e^- \gamma$ was similarly calculated to be 0.815%. With 15951 observed $K_L \rightarrow e^+ e^- \gamma$ events, and assuming branching ratios of 9.1×10^{-6} for $K_L \rightarrow e^+ e^- \gamma$, and 1.198% for $\pi^0 \rightarrow e^+ e^- \gamma$ [17], the single event sensitivity (SES) in this search was calculated to be $[2.56 \pm 0.02(\text{stat}) \pm 0.17(\text{sys})] \times 10^{-7}$. The statistical error comes from the statistics of $K_L \rightarrow e^+ e^- \gamma$ events. The systematic error represents the remaining errors, which are dominated by the uncertainty in $B(K_L \rightarrow e^+ e^- \gamma)$, 5.5%, and $B(\pi^0 \rightarrow e^+ e^- \gamma)$, 2.7%. The other contributions from the drift chamber's efficiency, TRD's efficiency, and the energy measurement were less than 1.9% each.

VI. CONCLUSION

Finally, we examined the signal region and found no events. Since no signal events were observed, the upper limit on the branching ratio of $K_L \rightarrow \pi^0 \nu \bar{\nu}$ at the 90% confidence level was determined to be $< 5.9 \times 10^{-7}$.

VII. FUTURE PROSPECTS FOR DALITZ METHOD

We define “background limit” as the SES at which, given indefinite running time, a given experiment would expect to observe one background event. This figure of merit shows the experimental potential for rare decay searches because it takes account not only a SES but also an expected background level. The “background limit” in this search is 3.1×10^{-8} . This is a factor of 49 lower than the “background limit” of Ref. [13], in which the SES is 4.04×10^{-7} with an expectation of 3.7 background events. Using the current detector and the beam, π_D^0 method has an advantage in the $K_L \rightarrow \pi^0 \nu \bar{\nu}$ search.

In future experiments, $\sim 10^{13}$ K_L decays are expected.

Using the Dalitz decay method, and assuming an experimental acceptance similar to that in the present result, the SES for $K_L \rightarrow \pi^0 \nu \bar{\nu}$ will be $\sim 10^{-9} \approx 1/(10^{13} \times 1.198\% \times 0.152\%)$. This is still two orders of magnitude above the standard model prediction. Therefore, in order to observe this decay at the predicted level in the next generation of kaon experiments, $\pi^0 \rightarrow \gamma\gamma$ decay mode will have to be used with improved beam and detector.

ACKNOWLEDGMENTS

We gratefully acknowledge the support and effort of the Fermilab staff and the technical staffs of the participating institutions for their vital contributions. This work was supported in part by the U.S. Department of Energy, The National Science Foundation and The Ministry of Education and Science of Japan. In addition, A.R.B., E.B., and S.V.S. acknowledge support from the NYI program of the NSF; A.R.B. and E.B. from the Alfred P. Sloan Foundation; E.B. from the OJI program of the U.S. DOE; K.H., T.N., and M.S. from the Japan Society for the Promotion of Science.

-
- [1] L.S. Littenberg, Phys. Rev. D **39**, 3322 (1989).
 - [2] J.S. Hagelin and L.S. Littenberg, Report No. MIU-THP-89/039, 1989.
 - [3] G. Buchalla and G. Isidori, Phys. Lett. B **440**, 170 (1998).
 - [4] J.L. Ritchie and S.G. Wojcicki, Rev. Mod. Phys. **65**, 1149 (1993).
 - [5] K. Hanagaki, Ph.D. thesis, Osaka University, 1998.
 - [6] D. Rein and L.M. Sehgal, Phys. Rev. D **39**, 3325 (1989).
 - [7] M. Kobayashi and T. Maskawa, Prog. Theor. Phys. **49**, 652 (1973); N. Cabibbo, Phys. Rev. Lett. **10**, 531 (1963).
 - [8] L. Wolfenstein, Phys. Rev. Lett. **51**, 1945 (1983).
 - [9] G. Buchalla and A.J. Buras, Nucl. Phys. **B400**, 225 (1993).
 - [10] P. Paganini, F. Parodi, P. Roudeau, and A. Stocchi, hep-ph/9711261 (1998); A.J. Buras, hep-ph/9711217 (1997).
 - [11] W.J. Marciano and Z. Parsa, Phys. Rev. D **53**, R1 (1996); G. Buchalla and A.J. Buras, *ibid.* **54**, 6782 (1996).
 - [12] Y. Grossman and Y. Nir, Phys. Lett. B **398**, 163 (1997); T. Hattori, T. Hasuike, and S. Wakaizumi, hep-ph/9804412, 1998.
 - [13] J. Adams *et al.*, Phys. Lett. B **447**, 240 (1999).
 - [14] E.D. Zimmerman, Nucl. Instrum. Methods Phys. Res. A **426**, 229 (1999).
 - [15] A. Roodman, in *Proceedings of the Seventh International Conference on Calorimetry in High Energy Physics*, edited by E. Cheu *et al.* (World Scientific, Singapore, 1998), p. 89.
 - [16] C. Bown *et al.*, Nucl. Instrum. Methods Phys. Res. A **369**, 248 (1996).
 - [17] Particle Data Group, C. Caso *et al.*, Eur. Phys. J. C **3**, 1 (1998).